Biol Trace Elem Res (2012) 147:366–373
DOI 10.1007/s12011-011-9297-1

Synthesis and Bioactive Studies of Complex 8-Hydroxyquinolinato-Bis-(Salicylato) Yttrium (III)

Xu Li · Qiang-Guo Li · Hui Zhang · Ji-Lin Hu · Fei-Hong Yao · De-Jun Yang · Sheng-Xiong Xiao · Li-Juan Ye · Yi Huang · Dong-Cai Guo

Received: 8 November 2011 / Accepted: 1 December 2011 / Published online: 14 December 2011

Abstract This paper reports the synthesis of a new bioactive complex, 8-hydroxyquinolinato-bis-(salicylato) yttrium (III) (HSAY), whose composition and structure were characterized by elemental analysis, IR spectra, thermogravimetric analysis, and X-ray diffraction. The power–time curves of the compounds HSAY, $C_7H_6O_3$, C_9H_7NO, and $YCl_3{\cdot}6H_2O$ on the growth metabolism of *Schizosaccharomyces pombe* (*S. pombe*) were determined at 32.00°C, respectively. The corresponding thermokinetics parameters, which include the microbial growth rate constant (κ), inhibition ratio (I), and half inhibition concentration (IC_{50}), were also derived. The results showed that the generation time was 168.2 min, and all the compounds HSAY, $C_7H_6O_3$, C_9H_7NO, and $YCl_3{\cdot}6H_2O$ possessed good bioactivities on the growth metabolism of *S. pombe*, with the values of IC_{50} being 0.055, 3.57, 0.057, and 1.35 mmol L^{-1}, respectively. The inhibition ability of these compounds above on the growth of the *S. pombe* has been observed to decrease in the order HSAY>C_9H_7NO>$YCl_3{\cdot}6H_2O$>$C_7H_6O_3$.

X. Li · Q.-G. Li (✉) · H. Zhang · J.-L. Hu · F.-H. Yao · D.-J. Yang · S.-X. Xiao · L.-J. Ye · Y. Huang
Department of Chemistry and Life Science, Xiangnan University, Chenzhou 423043, People's Republic of China
e-mail: liqiangguo@163.com

X. Li · Q.-G. Li · H. Zhang · J.-L. Hu · F.-H. Yao · D.-J. Yang · S.-X. Xiao · L.-J. Ye · Y. Huang
Hunan Provincial Key Laboratory of Xiangnan Rare-Precious Metals Compounds and Applications, Xiangnan University, Chenzhou 423043, People's Republic of China

D.-C. Guo
School of Chemistry and Chemical Engineering, Hunan University, Changsha 410082, People's Republic of China

Keywords 8-Hydroxyquinolinato-bis-(salicylato) yttrium (III) · Rare earth · *S. pombe* · Thermochemistry · Yttrium

Introduction

It is known that rare earth ions possess the properties of antibacterial [1], antitumor [2], and antivirus [3–5] agents when coordinated with organic small molecule ligands. Due to their strong affinities for many biological molecules, rare earth ions can effectively participate in many important life processes and activate or inhibit a variety of enzymes or proenzymes. For example, yttrium complexes exhibit some attractive bioactivities that are cytotoxic [6, 7] and antiproliferative [8–11]. Interestingly, recent reports showed that salicylic acid and its derivatives have potential anticancer [12, 13] and antibacterial [14] activities. In addition, complexing ligands such as 8-hydroxyquinoline and its derivatives were also reported to have promising bioactivities, including anticancer [15, 16], antibacterial [17, 18], antidyslipidemic and antioxidative properties [19], vasorelaxing properties [20], antivirus [21, 22], and antiplatelet [23] activities. Accordingly, the bioactivities of the product from the reaction of yttrium chloride hexahydrate with salicylic acid and 8-hydroxyquinoline could be expected to be significantly stronger than those of the yttrium ion, salicylic acid, and 8-hydroxyquinoline alone.

Biological microcalorimetry, providing a continuous measurement of heat production, can be employed to directly determine the biological activities of a living system. Heat flux is an expression of overall metabolic flux, and the detection of small changes in heat production to respond to toxic insult will be a sensitive indicator of altered metabolism. Since microcalorimetry is a nondestructive method with high accuracy and automaticity, it is now widely applied in biological research [24] and pharmacological analysis [25].

In this paper, we report the synthesis and characterization of the new bioactive complex, 8-hydroxyquinolinato-bis-(salicylato) yttrium (III) (HSAY). To further study the biological effects of HSAY and to clarify its pharmacological mechanisms, *Schizosaccharomyces pombe* (*S. pombe*) was used, as it provides an ideal model for studies in cell morphogenesis [26]. The interactions of HSAY with *S. pombe* were followed by means of microcalorimetry. The heat output power curve of metabolism of *S. pombe* was determined by a TAM Air calorimeter [27]. In addition, we analyzed the relationship between the concentration of HSAY and the growth of *S. pombe* by the thermokinetics model.

Experimental

Materials and Instrument

The microcalorimetric study was performed on a 3116-2/3239 TAM Air calorimeter (Thermometric AB, Sweden). Cell incubation was carried out in a temperature oscillation incubator (BS-1EA, China) and a carbon dioxide cell incubator (WJ-160A-II, China). The FT-IR spectrum was measured on an Avatar 360 FT-IR spectrometer (Thermo Nicalet Corporation, USA). Measurement of thermogravimetry (TG) and differential scanning calorimetry (DSC) curves was carried out on a NETZSCH STA449C thermal analysis instrument (NETZSCH Corporation, Germany). An elemental analyzer (Perkin-Elmer 2400 CHN, USA) was used to measure the C, H, and N contents of the complex. The conductivity monitor (DDS-12A, Shanghai, China) was used to measure the conductance of the complex. X-ray diffraction patterns were recorded on a D8 Advance X-ray diffractometer (Bruker Corporation, Germany).

S. pombe (ACCC 20047) was provided by Agricultural Culture Collection of China. The Edinburgh minimal medium (EMM) culture composition was K_2HPO_4 3 g, Na_2HPO_4 2.2 g, NH_4Cl 5 g, and glucose 20 g; the yeast extract medium composition was 20 mL and H_2O 1,000 mL (natural pH).

The chemicals $YCl_3{\cdot}6H_2O$(s) (>99%), $C_7H_6O_3$(s) (>99.5%), and C_9H_7NO(s) (>99.5%) were purchased from Shanghai Reagent Company. $YCl_3{\cdot}6H_2O$(s) was dried in a desiccator containing sulfuric acid (60%) at room temperature. $C_7H_6O_3$(s) and C_9H_7NO(s) were dried in a vacuum desiccator containing P_4O_{10} until their mass remained constant.

Synthesis and Characterization of the Complex

Synthesis of the Complex

8-Hydroxyquinolinato-bis-(salicylato) yttrium (III) was prepared according to the literature method [28]. A mass of 0.02 mol of powdered $C_7H_6O_3$ (s) was dissolved in 40 cm^3 of absolute ethyl alcohol (solution A). Sodium salicylate solution (solution B) was formed when an aqueous solution of 10% NaOH (0.02 mol NaOH) was added into the solution A. A mass of 0.01 mol of powdered 8-hydroxyquinoline was dissolved in 40 cm^3 of absolute ethyl alcohol (solution C). A mixture solution (solution D) was obtained when the solution B was added into the solution C. A mass of 0.01 mol of powdered $YCl_3{\cdot}6H_2O$ was dissolved in 40 cm^3 of anhydrous ethyl alcohol (solution E). Primrose yellow crystals were separated out when the solution E was added slowly into the solution D at 37.5°C after 3 h of magnetic stirring. The reaction solution was left to settle down at pH=6.5 to 7.0 for 12 h. Finally, the primrose yellow solid complex was obtained by vacuum filtration and successively washed with distilled water, absolute ethyl alcohol, and acetone several times. The product was put into a vacuum desiccator at 85°C for 24 h and kept until the mass of the crystals became constant.

Characterization of the Complex

The complex is obtained as a yellow solid. It is soluble in dimethyl formamide (DMF) and dimethyl sulfoxide (DMSO). A few of it can be dissolved in absolute ethyl alcohol but it cannot be dissolved in water, acetone, aether, and benzene. The molar conductance of the complex in DMF is 4.1×10^{-4} S m^2 mol^{-1}, indicating that the complex is a nonelectrolyte and exists as a neutral molecule in DMF.

The chemical composition of the synthetic complex was determined by elemental analysis for C, H, and N, by the EDTA titration for Y^{3+} [29], by mercury salt titration for Cl^-, and by TG-DSC curves for H_2O. The elemental analysis data [observed/percent (calculated/percent)], C 54.59 (54.46), H 3.08 (3.18), N 2.77 (2.76), and Y 17.47(17.52), showed that the composition of complex was $(C_7H_5O_3)_2Y(C_9H_6NO)$, and its purity was more than 99.8%.

Infrared spectra of the complex $(C_7H_5O_3)_2Y(C_9H_6NO)$, salicylic acid, and 8-hydroxyquinoline were obtained from KBr pellets at room temperature using an IR spectrophotometer. There are five characteristic bands observed for the salicylic acid: ν_{OH}^{COOH} (intramolecular hydrogen bond, 3,237 cm^{-1} s), ν_{OH}^{COOH} (intermolecular hydrogen bond, 2,857 cm^{-1} s), ν_{O-H} (COOH, 2,598 cm^{-1} s), ν_{C-O} (COOH, 1,663 cm^{-1} vs), and δ_{O-H} (phenol, 1,483 cm^{-1} s). All these bands disappeared after the complex formation except the band due to the angular deformation of the OH group. At the same time, two new absorption bands due to the carboxylate group $\nu_{as}^{COO^-}$ (1,593 cm^{-1}, s) and $\nu_{s}^{COO^-}$ (1,389 cm^{-1}, s), appeared, indicating that the oxygen atoms of the carboxylate group were coordinated to the rare earth ion (Y^{3+}). The values of the splitting for the absorption bands of the valency vibration $\nu_{as}^{COO^-}$ and $\nu_{s}^{COO^-}$ are all $\Delta\nu(\nu_{as}-\nu_s)=$

204cm^{-1}. This $\Delta\nu$ is equivalent to the $\Delta\nu$ of sodium salicylate. Accordingly, from these results, it can be concluded that the carboxylate group was coordinated to the rare earth ion through two oxygen atoms, as a symmetrical bidentate ligand.

There are four characteristic absorption bands observed for free 8-hydroxyquinoline: ν_{O-H} (3,102 cm^{-1}), $\nu_{C=O}$ (1,095 cm^{-1}), $\nu_{C=N}$ (1,579 cm^{-1}), and δ_{O-H} (1,224 cm^{-1}). Both of the two characteristic absorption bands ν_{O-H} (3,102 cm^{-1}) and δ_{O-H} (1,224 cm^{-1}) disappeared after formation of the coordinate complex; and meanwhile, $\nu_{C=O}$ (1,095 cm^{-1}) shifted towards higher frequency, increasing by 9 to 11 cm^{-1}, which may due to the rare earth ion (Y^{3+}) was coordination with ligands and form a Y–O bond in which the electronegativity of rare earth ion is less than that of hydrogen, while the electronegativity of oxygen is larger. In addition, the original absorption band $\nu_{C=N}$ (1,579 cm^{-1}) shifted towards lower frequency, decreasing by 7 to 10 cm^{-1}. From these results, we can conclude that the rare earth ion (Y^{3+}) was coordinated with the hydroxyl oxygen atom and hetero-nitrogen atom in 8-hydroxyquinoline, as a five-membered chelate ring. The chemical structure of the complex is given in Fig. 1.

TG and DSC curves of $(C_7H_5O_3)_2Y(C_9H_6NO)$ in the temperature range of room temperature to 1,320°C at a heating rate of 10°C min^{-1} in flowing N_2 are shown in Fig. 2. The thermal decomposition process of $(C_7H_5O_3)_2Y(C_9H_6NO)$ can be divided into three stages. The first stage is from 389°C to 540°C. The TG curve shows that the mass loss corresponding to this temperature range is 25.89%, which roughly coincides with the value of 26.84%, calculated for the loss of 1 mol of $(C_9H_6NO)^-$ from the complex. The second stage ranges from 621°C to 710°C with the mass loss of 33.36%, which corresponds to the loss of 1 mol of $(C_7H_5O_3)^-$. The theoretical mass loss is 34.79%. The third stage degradation temperature is in the range of 710°C to 992°C with the mass loss of 52.60%, which corresponds to the loss of 1 mol of $(C_7H_5O_3)^-$. The theoretical mass loss is 53.35%. On the basis of experimental and

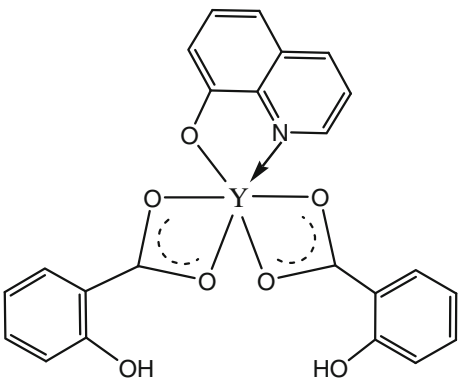

Fig. 1 Chemical structure of the complex

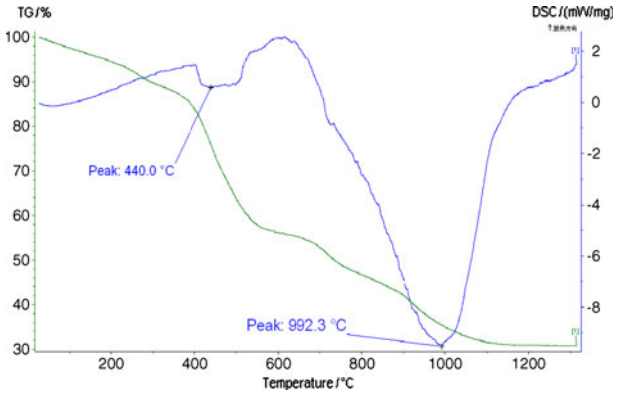

Fig. 2 TG-DSC curves of $(C_7H_5O_3)_2Y(C_9H_6NO)$

calculated results, the thermal decomposition of $(C_7H_5O_3)_2Y(C_9H_6NO)$ can be postulated as follows:

$$2(C_7H_5O_3)_2Y(C_9H_6NO) \xrightarrow{(389\text{ to }540)^\circ C} [Y(C_8H_5O_3)]_2O \xrightarrow{(621\text{ to }710)^\circ C} 2Y(C_7H_5O_3)O \xrightarrow{(710\text{ to }992)^\circ C} Y_2O_3.$$

X-ray diffraction measurement was performed on a D8 ADVANCE X-ray diffraction apparatus (Bruker Corporation, Germany) scanning from 5° to 80° using Cu Kα (λ= 1.54187 Å) radiation. The tube voltage was 40 KV, tube current was 40 mA, scanning speed was 0.5 s, and scanning step was 0.02°. The details of the XRD analysis results are shown in Fig. 3. According to the standard card (no. 33-1954) in a spectral database, it was demonstrated that the crystal type of $(C_7H_5O_3)_2Y(C_9H_6NO)$ was similar to that of $C_5H_{11}NO_2$. The cell parameters were a=5.426 nm, b=22.105 nm, and c=5.277 nm.

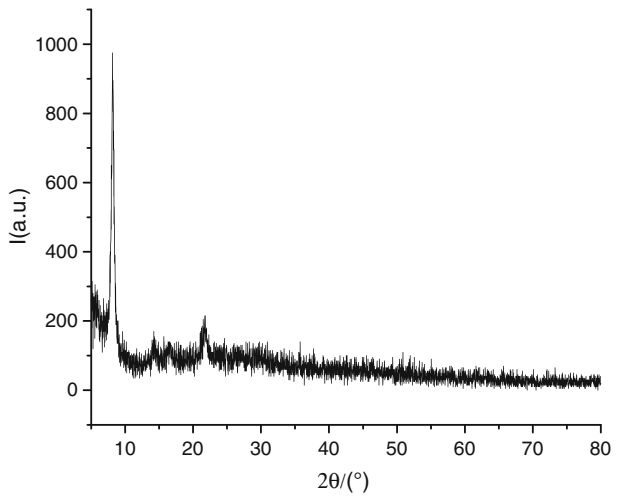

Fig. 3 XRD curve of $(C_7H_5O_3)_2Y(C_9H_6NO)$

Determination of Bioactivity of HSAY on *S. pombe* Cells by Biocalorimetry

The microcalorimetric measurements were carried out on a TAM air isothermal microcalorimeter at 32.00°C. Baselines were taken before each measurement and the calorimeter was calibrated electrically. More details of the performance and construction of the instrument are available in [27].

When the system had gained a stable baseline, 5 mL EMM-sterilized culture medium was added into the sterilized sample ampoules. *S. pombe* was inoculated with an initial density of 1×10^6 cells·mL^{-1}. Samples of HSAY at different concentrations were added to the cell suspension, respectively. Power–time curves for all measurements were performed at 32.00°C. All the microcalorimetric experiments were repeated three times and the results were identical.

Results and Discussion

Thermogenic Curves

The thermogenic curves for growth of *S. pombe* cells treated by different concentrations of the compounds HSAY, $C_7H_6O_3$, C_9H_7NO, and $YCl_3\cdot6H_2O$ were determined by using the ampoule method at 32.00°C, respectively. All microcalorimetric experiments were repeated three times. The results are illustrated in Fig. 4. From Fig. 4, we can find that the thermogenic curves are similar to those of *S. pombe* treated by different concentrations of HSAY. As shown as in Fig. 4a, the metabolic process can be divided into four phases: lag phase (AB), activity recovery phase (BC), stationary phase (CD), and decline phase (DE). Figure 4 obviously revealed that all the compounds HSAY, $C_7H_6O_3$, C_9H_7NO, and $YCl_3\cdot6H_2O$ possessed the bidirectional biological effect and Hormesis effect. They stimulated

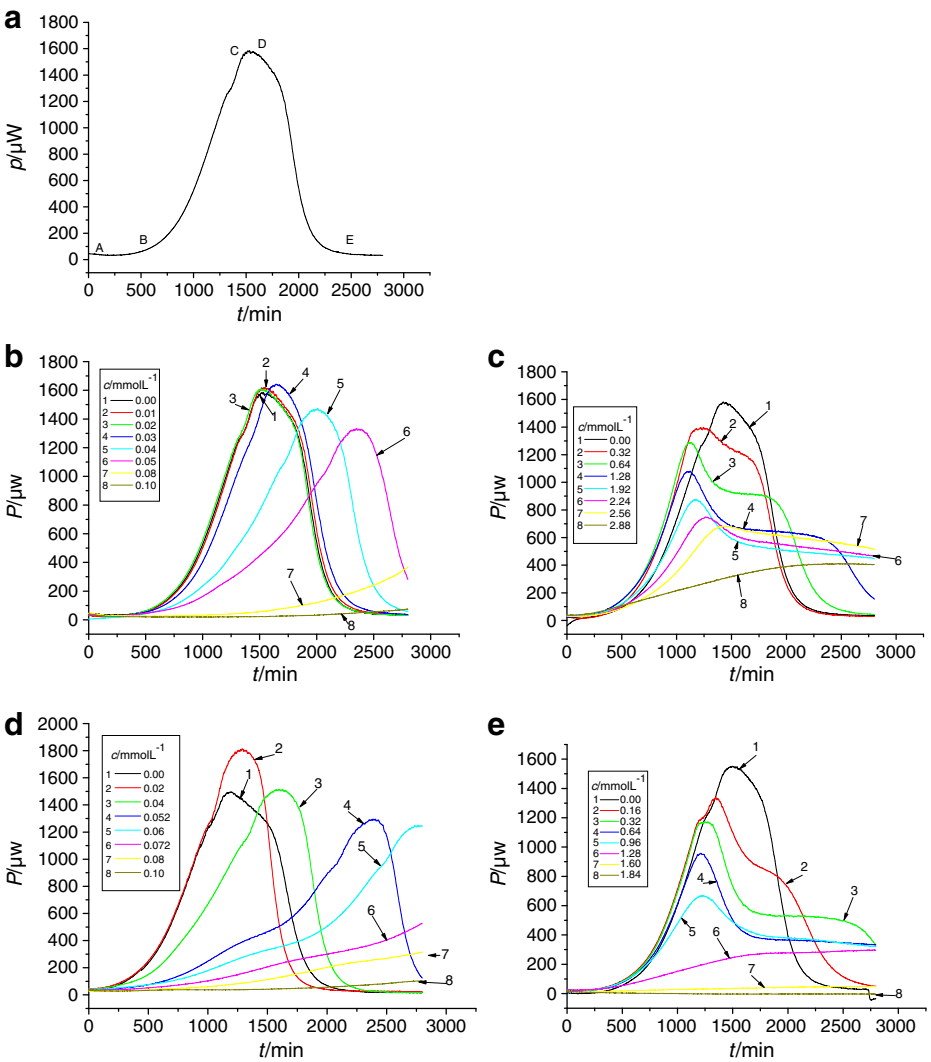

Fig. 4 Metabolically thermogenic curves of *S. pombe* cells affected by the complex and ligands at 32.00°C. **a** Control; **b** HSAY; **c** $C_7H_6O_3$; **d** C_9H_7NO; **e** $YCl_3\cdot6H_2O$

the growth of the *S. pombe* at low concentration, but inhibited the growth of *S. pombe* at high concentration.

Thermokinetics

During the lag phase of Fig. 4, the power–time curves obeyed the following equation:

$$\ln P_t = \ln P_0 + kt \quad (1)$$

where P_t was the heat output power of the *S. pombe* cell at time t, and k was the growth rate constant of the *S. pombe* cell at specified conditions, whose size represented growth speed. Using this equation, the growth rate constant k could be calculated and the results are shown in Table 1.

Plot of the growth rate constant (k) against concentration (c) is shown in Fig. 5. It could be seen from Fig. 5 that the growth rate constant (κ) of *S. pombe* slightly increased with the increasing of the concentration of HSAY among the range of 0.00 to 0.01 mmol L^{-1}, while it decreased with the increasing of the concentration of HSAY among the range of 0.01 to 0.10 mmol L^{-1}, which showed the HSAY possessed the bidirectional biological effect and Hormesis effect that was HSAY stimulated the growth of *S. pombe* at low concentration, but inhibited the growth of *S. pombe* at high concentration. The relationship between κ and c_{HSAY} could be described as:

$$\kappa = 0.00679 - 1.16 \times 10^{-4} / \left(4(c - 0.09463)^2 + 0.14185^2\right) \quad \left(0.01\ \text{mmol}\,L^{-1} \le c_{HSAY} \le 0.10\ \text{mmol}\,L^{-1}\right). \quad (2)$$

Table 1 Thermokinetics parameters of the growth of *S. pombe* affected by HSAY, $YCl_3 \cdot 6H_2O$, $C_7H_6O_3$, and C_9H_7NO at different concentrations at 32.00°C

Inhibitors	C/mmol L^{-1}	k/min^{-1}	I/%	IC_{50}/mmol L^{-1}	$Q_{total/J}$
Control HSAY	0.00	$4.12\times10^{-3}\pm5.0\times10^{-5}$[a]	0.00		84.61
	0.01	$4.19\times10^{-3}\pm5.3\times10^{-5}$	−1.70		85.92
	0.02	$4.15\times10^{-3}\pm4.5\times10^{-5}$	−0.73		85.92
	0.03	$3.85\times10^{-3}\pm5.5\times10^{-5}$	6.55		84.91
	0.04	$3.30\times10^{-3}\pm5.6\times10^{-5}$	19.90		84.09
	0.05	$2.25\times10^{-3}\pm6.5\times10^{-5}$	45.39	0.055	81.85
	0.08	$1.35\times10^{-3}\pm5.6\times10^{-5}$	67.23		16.20
	0.10	$9.75\times10^{-4}\pm6.7\times10^{-5}$	76.33		5.20
Control $C_7H_6O_3$	0.00	$4.12\times10^{-3}\pm1.5\times10^{-5}$	0.00		85.67
	0.64	$4.30\times10^{-3}\pm1.6\times10^{-5}$	−4.37		83.90
	1.28	$4.22\times10^{-3}\pm1.5\times10^{-5}$	−2.43		85.90
	1.92	$4.15\times10^{-3}\pm1.5\times10^{-5}$	−0.73		85.21
	2.24	$3.72\times10^{-3}\pm1.1\times10^{-5}$	9.71		73.31
	2.56	$3.37\times10^{-3}\pm1.6\times10^{-5}$	18.20		70.78
	2.88	$2.90\times10^{-3}\pm1.8\times10^{-5}$	29.61		70.47
	3.68	$1.94\times10^{-3}\pm2.0\times10^{-5}$	52.91	3.57	44.89
Control C_9H_7NO	0.00	$4.13\times10^{-3}\pm5.8\times10^{-5}$	0.00		83.73
	0.02	$4.14\times10^{-3}\pm5.5\times10^{-5}$	−0.24		82.71
	0.04	$3.29\times10^{-3}\pm5.6\times10^{-5}$	20.34		83.44
	0.052	$2.37\times10^{-3}\pm6.6\times10^{-5}$	42.62	0.057	80.32
	0.06	$1.65\times10^{-3}\pm6.4\times10^{-5}$	60.05		67.91
	0.072	$1.40\times10^{-3}\pm5.2\times10^{-5}$	66.10		34.39
	0.08	$1.15\times10^{-3}\pm6.2\times10^{-5}$	72.15		21.91
	0.10	$6.95\times10^{-4}\pm7.2\times10^{-5}$	83.17		8.39
Control $YCl_3 \cdot 6H_2O$	0.00	$4.12\times10^{-3}\pm4.5\times10^{-5}$	0.00		82.26
	0.16	$4.33\times10^{-3}\pm6.0\times10^{-5}$	−4.85		83.31
	0.32	$4.41\times10^{-3}\pm6.0\times10^{-5}$	−7.04		80.38
	0.64	$4.22\times10^{-3}\pm6.5\times10^{-5}$	−2.43		60.03
	0.96	$3.90\times10^{-3}\pm5.6\times10^{-5}$	5.34		55.09
	1.28	$2.34\times10^{-3}\pm7.2\times10^{-5}$	43.20	1.35	31.75
	1.60	$8.50\times10^{-4}\pm7.6\times10^{-5}$	79.37		5.41
	1.84	0	100		0

c concentration, k growth rate constant of *S. pombe*, I inhibitive ratio, IC_{50} half inhibition concentration, Q_{total} total thermal effect

[a]Mean±SD; n=3

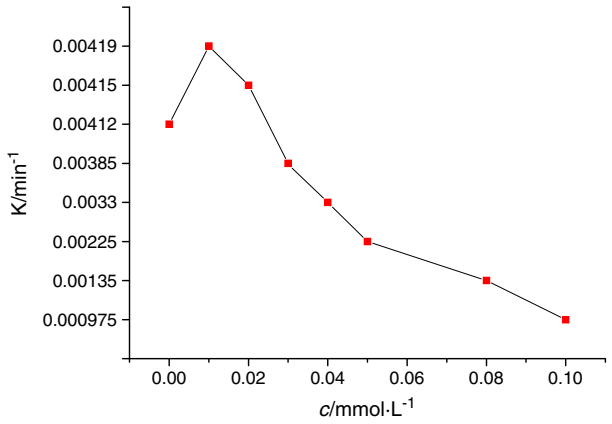

Fig. 5 Rate constant of growth k of *S. pombe* with different concentrations of HSAY

The correlation coefficient R was 0.9862. Thus, the growth rate constant (k) in the range of the above applied amount of HSAY on *S. pombe* could be clearly inferred through the application of Eq. 2.

The generation time can be calculated as: $t_G = \ln 2/k = 168.2\,\text{min}$.

The inhibition ratio of the growth metabolism of *S. pombe* cells by drug was defined as following:

$$I = \frac{(\kappa_0 - \kappa_c)}{\kappa_0} \times 100\% \quad (3)$$

where k_0 was the control rate constant (without any drug inhibition) of *S. pombe* and k_c was the growth rate constant of *S. pombe* under an inhibitor with a concentration of c. The values of (I) are shown in Table 1. When the inhibition ratio was 50%, the drug concentration was the half inhibition concentration (IC_{50}).

By plotting the inhibition ratio (I) against concentration (c), Fig. 6 was obtained. It could be seen that the inhibition ratio (I) was gradually increased with the increasing of concentration (c) of HSAY, which indicated that the growth of *S. pombe* was significantly inhibited. Using the Lorentz curve fitting the data of the inhibition ratio (I) of *S. pombe* with concentration (c) of HSAY, the curve equation was obtained:

$$I = -36.667 + 1.4166/\left(4(c - 0.09322)^2 + 0.11176^2\right) \quad \left(0.01\,\text{mmol}\,\text{L}^{-1} \le c_{\text{HSAY}} \le 0.10\,\text{mmol}\,\text{L}^{-1}\right). \quad (4)$$

The correlation coefficient R was 0.9813. Thus, the inhibition ratio in the range of the above applied amount of HSAY on *S. pombe* could be clearly inferred through the application of Eq. 4. The half inhibition concentrations (IC_{50}) of HSAY, $C_7H_6O_3$, C_9H_7NO, and $YCl_3{\cdot}6H_2O$ were found to be 0.055, 3.57, 0.057, and 1.35 mmol L^{-1}, respectively. The inhibition ability of these compounds above on the growth of the *S. pombe* has been observed to decrease in the order TSAS>C_9H_7NO>$YCl_3{\cdot}6H_2O$>$C_7H_6O_3$. The inhibitory action of the complex HSAY was greatly stronger than that of the two ligands ($C_7H_6O_3$ and C_9H_7NO) and $YCl_3{\cdot}6H_2O$ alone. From the above-mentioned results, a conclusion can be reached that the compound HSAY could be a good inhibitor on the bacteria and the tumor cells.

Thermodynamics

The total thermal effect (Q_{total}) value can be calculated by the area under the power–time curves and shown in Table 1. Where the heat output has been observed to remain almost the same and the mean value can be obtained.

The curve in Fig. 7 shows the plotting of the total thermal effect (Q_{total}) of *S. pombe* growth against concentration (c).

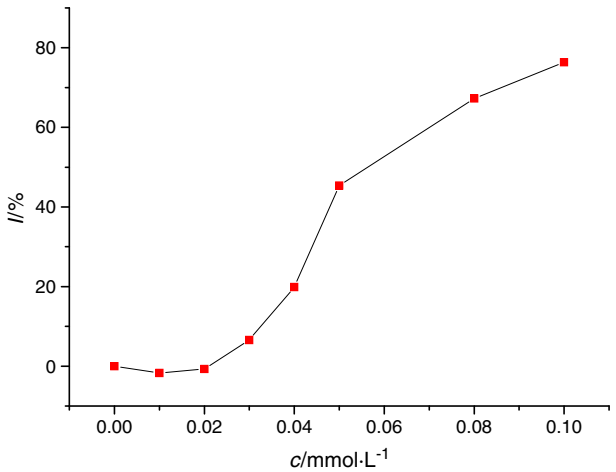

Fig. 6 The relationship between drug concentration c and the growth inhibition rate (I) of *S. pombe*

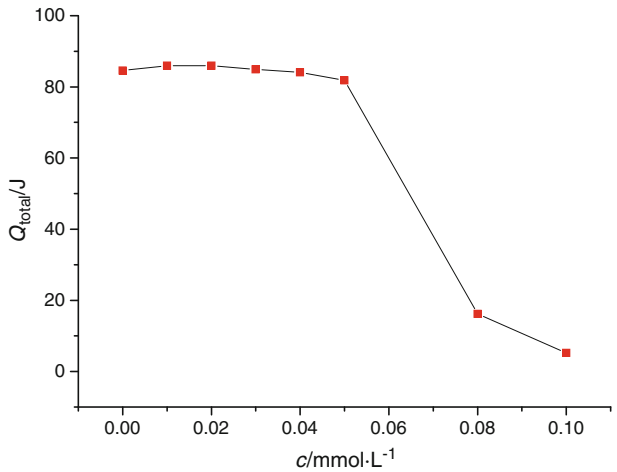

Fig. 7 Total thermal effect (Q_{total}) of *S. pombe* with different concentrations of HSAY

By using the Gauss curve fitting the data of the total thermal effect (Q_{total}) of *S. pombe* growth with concentration of HSAY (c), the curve equation was obtained:

$$Q_{total} = 85.268 - 89.91 \times \exp\left(-2 \times (c - 0.09203)/0.03311\right)^2$$

$$(0.01\,\text{mmol}\,\text{L}^{-1} \le c_{HSAY} \le 0.10\,\text{mmol}\ \text{L}^{-1}) \qquad (5)$$

The correlation coefficient R was 0.9999. Thus, the total thermal effect in the range of the above applied amount of HSAY on *S.pombe* could be clearly inferred through the application of Eq. 5. From Fig. 7, it could be seen that under low concentration of HSAY, the total thermal effect (Q_{total}) of *S. pombe* growth augmented with the increasing of the concentration of HSAY, which indicated that HSAY ratherish stimulated the growth of *S. pombe* cell; while under high concentration, the total thermal effect (Q_{total}) of *S. pombe* growth decreased with increasing of the concentration of HSAY, which indicated that HSAY significantly inhibited the growth of *S. pombe* cell.

Conclusions

In this work, a new bioactive complex, 8-hydroxyquinolinato-bis-(salicylato) yttrium (III) (HSAY), was synthesized and characterized. The experimental results indicated that HSAY possessed the bidirectional biological effect and Hormesis effect. HSAY stimulated the growth of the *S. pombe* at low concentration, but inhibited the growth of the *S. pombe* at high concentration. The half inhibition concentrations (IC_{50}) of HSAY, $C_7H_6O_3$, C_9H_7NO, and $YCl_3{\cdot}6H_2O$ were found to be 0.055, 3.57, 0.057, and 1.35 mmol L^{-1}, respectively. The inhibition ability of these compounds on the growth of the *S. pombe* has been observed to decrease in the order HSAY>C_9H_7NO>$YCl_3{\cdot}6H_2O$>$C_7H_6O_3$.

The present study demonstrates that microcalorimetry is a valuable tool for studies of *S. pombe* because it could provide important thermokinetics and thermodynamic information that cannot be obtained from conventional biological techniques. In conclusion, the present work provides new insights for the biothermochemical studies of HSAY on *S. pombe* and has theoretical and practical significance for the life science.

Acknowledgments This research was financially supported by the National Natural Science Foundation of China (no. 20973145), the Hunan Provincial Natural Science Foundation (no. 08JJ3014) of China, and the Hunan Provincial Educational Ministry Foundation of China (no. 06C784). The authors would like to gratefully acknowledge Master Hui-Wen Gu (State Key Laboratory of Chemo/Biosensing & Chemometrics, Hunan University, People's Republic of China) for his help in reviewing and revising our manuscript. Prof. Qiang-Guo Li would like to thank Dr. Qing-Qi Chen (MedKoo Biosciences, Inc, USA) for his help in preparing this manuscript.

References

1. Yang L, Tao D, Yang X, Li Y, Guo Y (2003) Synthesis, characterization, and antibacterial activities of some rare earth metal complexes of pipemidic acid. Chem Pharm Bull(Tokyo) 51:494–502
2. Zhou J, Wang LF, Wang JY, Tang N (2001) Synthesis, characterization, antioxidative and antitumor activities of solid quercetin rare earth(III) complexes. J Inorg Biochem 83:41–49
3. De Gusseme B, Du Laing G, Hennebel T, Renard P, Chidambaram D, Fitts JP, Bruneel E, Van Driessche I, Verbeken K, Boon N, Verstraete W (2010) Virus removal by biogenic cerium. Environ Sci Technol 44:6350–6356
4. Liu YN, Shi S, Mei WJ, Tan CP, Chen LM, Liu J, Zheng WJ, Ji LN (2008) In vitro and in vivo investigations on the antiviral activity of a series of mixed-valence rare earth borotungstate heteropoly blues. Eur J Med Chem 43:1963–1970
5. Manolov I, Raleva S, Genova P, Savov A, Froloshka L, Dundarova D, Argirova R (2006) Antihuman immunodeficiency virus type 1 (HIV-1) activity of rare earth metal complexes of 4-hydroxycoumarins in cell culture. Bioinorg Chem Appl 2006:71938
6. Saturnino C, Napoli M, Paolucci G, Bortoluzzi M, Popolo A, Pinto A, Longo P (2010) Synthesis and cytotoxic activities of group 3 metal complexes having monoanionic tridentate ligands. Eur J Med Chem 45:4169–4174
7. Hou AX, Liu Y, Wong WK, Xue Z, Qu SS (2003) Interaction of Y^{3+} and its cationic monoporphyrinate complex with *Staphylococcus aureus*. Acta Chim Sin 61:1382–1387
8. Kostova I, Trendafilova N, Momekov G (2008) Theoretical, spectral characterization and antineoplastic activity of new lanthanide complexes. J Trace Elem Med Biol 22:100–111
9. Kostova I, Kostova R, Momekov G, Trendafilova N, Karaivanova M (2005) Antineoplastic activity of new lanthanide (cerium, lanthanum and neodymium) complex compounds. J Trace Elem Med Biol 18:219–226
10. Kostova I, Manolov I, Nicolova I, Konstantinov S, Karaivanova M (2001) New lanthanide complexes of 4-methyl-7-hydroxycoumarin and their pharmacological activity. Eur J Med Chem 36:339–347
11. Zhu WZ, Lin QY, Lu M, Hu RD, Zheng XL, Cheng JP, Wang YY (2009) Synthesis, characterization, DNA-binding and antiproliferative activity of Nd(III) complexes with N-(nitrogen heterocyclic) norcantharidin acylamide acid. J Fluoresc 19:857–866
12. Stark LA, Reid K, Sansom OJ, Din FV, Guichard S, Mayer I, Jodrell DI, Clarke AR, Dunlop MG (2007) Aspirin activates the NF-kappaB signalling pathway and induces apoptosis in intestinal neoplasia in two in vivo models of human colorectal cancer. Carcinogenesis 28:968–976
13. Price CT, Lee IR, Gustafson JE (2000) The effects of salicylate on bacteria. Int J Biochem Cell Biol 32:1029–1043
14. Shaw AY, Chang CY, Hsu MY, Lu PJ, Yang CN, Chen HL, Lo CW, Shiau CW, Chern MK (2010) Synthesis and structure-activity relationship study of 8-hydroxyquinoline-derived Mannich bases as anticancer agents. Eur J Med Chem 45:2860–2867
15. Shen AY, Wu SN, Chiu CT (1999) Synthesis and cytotoxicity evaluation of some 8-hydroxyquinoline derivatives. J Pharm Pharmacol 51:543–548
16. Ding WQ, Liu B, Vaught JL, Yamauchi H, Lind SE (2005) Anticancer activity of the antibiotic clioquinol. Cancer Res 65:3389–3395
17. Darby CM, Nathan CF (2010) Killing of non-replicating *Mycobacterium tuberculosis* by 8-hydroxyquinoline. J Antimicrob Chemother 65:1424–1427
18. Ibrahim SA, Makhlouf MT, Abdel-Hafez AA, Moharram AM (1986) Some transition metal chelates of 8-hydroxyquinoline-5-sulfonamides as possible drugs. J Inorg Biochem 28:57–65

19. Kay K (1978) The use of 8-hydroxyquinoline hydrochloride as a dental antibacterial agent. J Periodontol 49:47
20. Sashidhara KV, Kumar A, Bhatia G, Khan MM, Khanna AK, Saxena JK (2009) Antidyslipidemic and antioxidative activities of 8-hydroxyquinoline derived novel keto-enamine Schiffs bases. Eur J Med Chem 44:1813–1818
21. Bertini S, Calderone V, Carboni I, Maffei R, Martelli A, Martinelli F, Minutolo Rajabi M, Testai L, Tuccinardi T, Ghidoni R, Macchia M (2010) Synthesis of heterocycle-based analogs of resveratrol and their antitumor and vasorelaxing properties. Bioorg Med Chem 18:6715–6724
22. Liu YJ, Zhao Y, Zhai X, Feng X, Wang J, Gong P (2008) Synthesis and anti-hepatitis B virus evaluation of novel ethyl 6-hydroxyquinoline-3-carboxylates in vitro. Bioorg Med Chem 16:6522–6527
23. Zeng XW, Huang N, Xu HY, Yang WB, Yang LM, Qu H, Zheng YT (2010) Anti human immunodeficiency virus type 1 (HIV-1) agents 4. Discovery of 5,5'-(p-phenylenebisazo)-8-hydroxyquinoline sulfonates as new HIV-1 inhibitors in vitro. Chem Pharm Bull (Tokyo) 58:976–979
24. Montanari MLC, Beezer AE, Montanari CA, Pilo-Veloso D (2000) QSAR based on biological microcalorimetry. J Med Chem 43:3448–3452
25. Urakami K (2005) Characterization of pharmaceutical polymorphs by isothermal calorimetry. Curr Pharm Biotechnol 6:193–203
26. Juan Cortes JC, Carnero E, Ishiguro J, Sánchez Y, Durán A, Ribas JC (2005) The novel fission yeast (1,3)beta-D-glucan synthase catalytic subunit Bgs4p is essential during both cytokinesis and poSmrized growth. J Cell Sci 118(Pt 1):157–174
27. Li QG, Yang DJ, Li X, Ye LJ, Wei DL, Xiao SX (2008) Thermokinetic studies of action of complexes $[RE(Hsal)_2\text{-}(tch)]\text{-}2H_2O$ on growth metabolism of *Escherichia Coli*. Acta Chim Sin 66:2686–2692
28. Li QG, Huang Y, Li X, Ye LJ, Xiao SX, Yang DJ, Liu Y (2008) Synthesis, characterization and standard molar enthalpy of formation of $Nd(C_7H_5O_3)_2$ (C_9H_6NO). J Therm Anal Cal 91:615–620
29. Xie ZQ (1985) Determination of center lanthanide ions in organic complex salts. J Wuhan Univ 2:117–122